American Concrete Institute
Always advancing

Unconventional Reinforced Concrete Bridge Columns

ACI Spring 2014 Convention
March 23 - 25, Reno, NV

Ahmed Al-Rahmani earned his MS in Structural Engineering form Kansas State University. He is currently a Ph.D student of Structural Engineering at the same institute. His research interests include finite element analysis, artificial neural networks and concrete confinement modeling.

ACI Spring 2014 Convention

Concentric and Eccentric Behavior of Rectangular Columns Confined by Steel Ties and FRP Wrapping

Ahmed Al-Rahmani
Dr. Hayder Rasheed

Department of Civil Engineering
Kansas State University

Outline

- Objectives.
- Introduction.
- Formulation.
- Computer Program.
- Results.
- Summary and Conclusions.

4

Objectives

- Evaluate the proposed model which combines steel and FRP confinement effect in rectangular concrete columns.
- Generate interaction diagrams for these columns accounting for this confinement effect.

5

Introduction

- Many models were proposed to describe the FRP confinement effect.
  - Lam and Teng model was found to be the most suitable*.
- Reinforced Concrete columns are subject to two different confining pressure from steel and FRP.
- This study proposes a new model that combines both FRP and steel confinement.

*ACI Committee 440-F Task Group Report on FRP Confinement (January 2007)

6

Formulation

- Generalized Moment of Area Theorem.
- Mander Model (Steel Confinement).
- Lam and Teng Model (FRP Confinement).
- Combined Confinement Model (Steel and FRP).
- Eccentricity-Based Models.
- Confined Analysis Procedure.

7

Generalized Moment of Area Theorem

$$\sigma_z = \frac{P}{A} + \frac{M_x I_y - M_y I_{xy}}{I_x I_y - I_{xy}^2} y + \frac{M_y I_x - M_x I_{xy}}{I_x I_y - I_{xy}^2} x$$

$$\varepsilon_z = \frac{P}{EA} + \frac{M_x EI_y - M_y EI_{xy}}{EI_x EI_y - EI_{xy}^2} y + \frac{M_y EI_x - M_x EI_{xy}}{EI_x EI_y - EI_{xy}^2} x$$

$$\phi_x = \frac{M_x EI_y - M_y EI_{xy}}{\beta^2} \qquad \phi_y = \frac{M_y EI_x - M_x EI_{xy}}{\beta^2}$$

$$\varepsilon_z = \frac{P}{EA} + \phi_x y + \phi_y x$$

At geometric centroid

$$P = EA\overline{\varepsilon_o} - EA\bar{y}\phi_x - EA\bar{x}\phi_y \qquad \boxed{P = EA\overline{\varepsilon_o} - EAM_x\phi_x - EAM_y\phi_y}$$

8

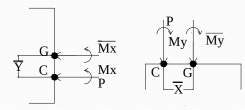

$$\overline{M_x} = M_x - P\bar{y} \qquad \overline{M_y} = M_y - P\bar{x}$$

$$M_x = EI_x\phi_x + EI_{xy}\phi_y \qquad M_y = EI_{xy}\phi_x + EI_y\phi_y$$

$$\boxed{\overline{M_x} = EI_x\phi_x + EI_{xy}\phi_y - EA\overline{\varepsilon_o}\,\bar{y} + EAM_x\phi_x\bar{y} + EAM_y\phi_y\bar{y}}$$

$$\boxed{\overline{M_y} = -EAM_y\overline{\varepsilon_o} + \left(EI_{xy} + EAM_x\bar{x}\right)\phi_x + \left(EI_y + EAM_y\bar{x}\right)\phi_y}$$

9

$$\begin{bmatrix} P \\ \overline{M_x} \\ \overline{M_y} \end{bmatrix} = \begin{bmatrix} EA & -EAM_x & -EAM_y \\ -EAM_x & EI_x & EI_{xy} \\ -EAM_y & EI_{xy} & EI_y \end{bmatrix} \begin{bmatrix} \varepsilon \\ \phi_x \\ \phi_y \end{bmatrix}$$

$$\begin{bmatrix} P \\ M_x \\ M_y \end{bmatrix} = \begin{bmatrix} EA & 0 & 0 \\ 0 & EI_x & EI_{xy} \\ 0 & EI_{xy} & EI_y \end{bmatrix} \begin{bmatrix} \varepsilon \\ \phi_x \\ \phi_y \end{bmatrix}$$

10

Mander Model

$$k_e = \frac{\left(1 - \sum_{i=1}^{n} \frac{(w_i')^2}{6b_c d_c}\right)\left(1 - \frac{s'}{2b_c}\right)\left(1 - \frac{s'}{2d_c}\right)}{(1 - \rho_{cc})}$$

$$\rho_x = \frac{A_{sx}}{2d_c}$$

$$\rho_y = \frac{A_{sy}}{2b_c}$$

$$f_{lx} = k_e \rho_x f_{yh}$$

$$f_{ly} = k_e \rho_y f_{yh}$$

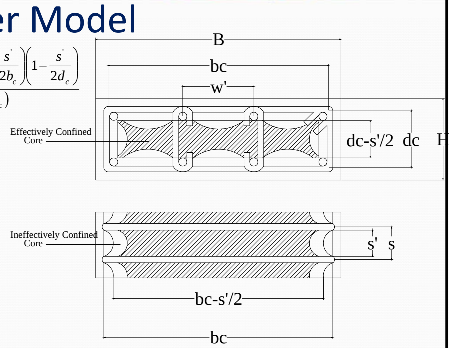

11

Mander Model

$$f_c = \frac{f_{cc} x r}{r - 1 + x^r}$$

$$x = \frac{\varepsilon_c}{\varepsilon_{cc}} \qquad r = \frac{E_c}{E_c - E_{sec}}$$

$$E_{sec} = \frac{f_{cc}}{\varepsilon_{cc}}$$

$$\varepsilon_{cc} = \varepsilon_{co}\left[1 + 5\left(\frac{f_{cc}}{f_c'} - 1\right)\right]$$

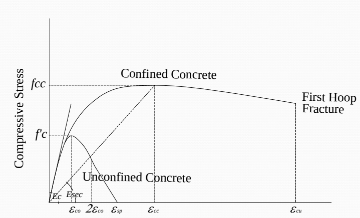

12

Lam and Teng Model

$$f_c = E_c\varepsilon_c - \frac{(E_c - E_2)^2}{4f_c'}\varepsilon_c^2 \quad 0 \le \varepsilon_c \le \varepsilon_t'$$

$$f_c = f_c' + E_2\varepsilon_c \quad \varepsilon_t' \le \varepsilon_c \le \varepsilon_{ccu}$$

$$E_2 = \frac{f_{cc}' - f_c'}{\varepsilon_{ccu}}$$

$$\varepsilon'_t = \frac{2f_c'}{E_c - E_2}$$

$$\varepsilon_{ccu} = \varepsilon_c'\left(1.50 + 12\kappa_b\frac{f_l}{f_c'}\left(\frac{\varepsilon_{fe}}{\varepsilon_c'}\right)^{0.45}\right) \quad \varepsilon_{ccu} \le 0.01$$

$$f_{lx} = \frac{2E_f n t_f \varepsilon_{fe}}{H} \quad f_{ly} = \frac{2E_f n t_f \varepsilon_{fe}}{B} \quad \varepsilon_{fe} = \kappa_\varepsilon\varepsilon_{fu}$$

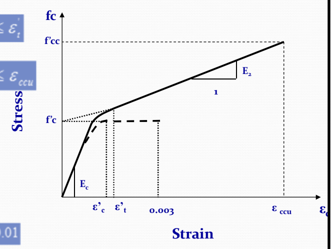

Combined Confinement Model

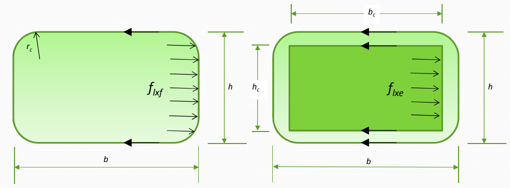

$$f_{lxf} = \frac{2nt_f E_f \varepsilon_{fe}}{h} \qquad f_{lxe} = \frac{2nt_f E_f \varepsilon_{fe}}{h} + k_e\rho_x f_{yh}$$

$$f_{lyf} = \frac{2nt_f E_f \varepsilon_{fe}}{b} \qquad f_{lye} = \frac{2nt_f E_f \varepsilon_{fe}}{b} + k_e\rho_y f_{yh}$$

14

- *Equivalent Circular Section:*
  - $D = \sqrt{b^2 + h^2}$
  - $f_{lf} = \frac{2nt_f E_f \varepsilon_{fe}}{D}$
- If $f_{lf}/f'_c > 0.08$:
  - Use Lam and Teng Model.
- If $f_{lf}/f'_c < 0.08$:
  - Use Mander Model.

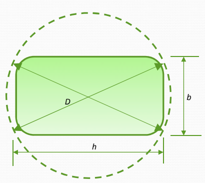

15

Determine f_{lx} and f_{ly}

Convert into negative values to represent the major and intermediate principal stresses (σ_1, σ_2) so that $\sigma_1 > \sigma_2$

Assume an initial value for f'_{cc}, the minor principal stress (σ_3)

Calculate σ_{oct}, τ_{oct} , and θ as follows:

$$\sigma_{oct} = \frac{1}{3}(\sigma_1 + \sigma_2 + \sigma_3) \qquad \tau_{oct} = \frac{1}{3}[(\sigma_1 - \sigma_2)^2 + (\sigma_2 - \sigma_3)^2 + (\sigma_1 - \sigma_3)^2]^{\frac{1}{2}} \qquad \cos\theta = \frac{\sigma_1 - \sigma_{oct}}{\sqrt{2}\tau_{oct}}$$

Determine the ultimate stress meridian surfaces, T and C as follows: (Elwy and Murray, 1979)

$$T = 0.069232 - 0.661091\overline{\sigma_{oct}} - 0.04935(\overline{\sigma_{oct}})^2 \qquad C = 0.122965 - 1.150502\overline{\sigma_{oct}} - 0.315545(\overline{\sigma_{oct}})^2 \qquad \overline{\sigma_{oct}} = \sigma_{oct}/f'_c$$

Determine τ_{oct} using the interpolation function (Willam and Warnke, 1975)

$$\overline{\tau_{oct}} = C\frac{0.5D/\cos\theta + (2T - C)(D + 5T^2 - 4TC)^{\frac{1}{2}}}{D + (2T - C)^2} \qquad D = 4(C^2 - T^2)\cos^2\theta \qquad \tau_{oct} = f'_c\overline{\tau_{oct}}$$

Recalculate f'_{cc} as follow:

$$\sigma_3 = \frac{\sigma_1 + \sigma_2}{2} - \sqrt{4.5\tau_{oct}^2 - 0.75(\sigma_1 - \sigma_2)^2}$$

16

Eccentric Model

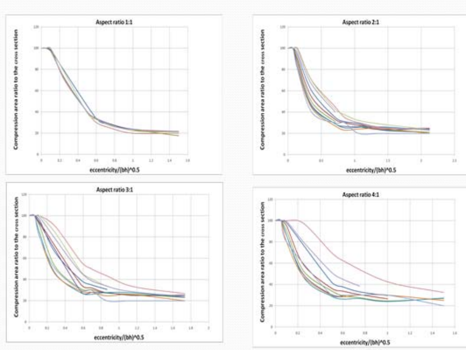

17

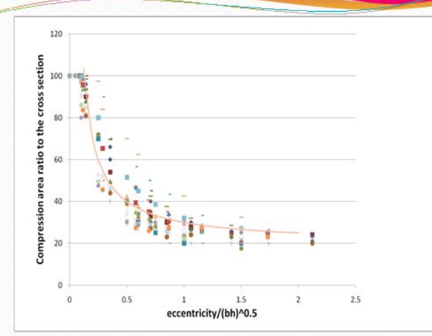

$$C_R = \frac{0.2 * \frac{e}{\sqrt{bh}} + 0.1}{\frac{e}{\sqrt{bh}}}$$

18

Mander Eccentricity Based Model

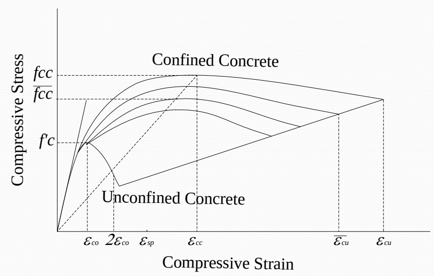

19

Mander Eccentricity Based Model

- $\overline{f_{cc}} = \frac{1}{1+\frac{1}{C_R-0.2}} f_{cc} + \frac{1}{0.8+C_R} f'_c$
- $\overline{\varepsilon_{cc}} = \varepsilon_{co}\left[1+5\left(\frac{\overline{f_{cc}}}{f'_c}-1\right)\right]$
- $f_c = \frac{\overline{f_{cc}}\, x\bar{r}}{\bar{r}-1+\bar{x}^{\bar{r}}}$
- $\bar{x} = \frac{\varepsilon_c}{\overline{\varepsilon_{cc}}}$
- $\bar{r} = \frac{E_c}{E_c-\overline{E_{sec}}}$
- $\overline{E_{sec}} = \frac{\overline{f_{cc}}}{\overline{\varepsilon_{cc}}}$

20

Lam & Teng Eccentricity Based Model

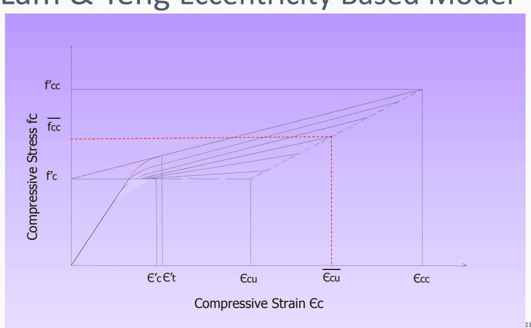

21

Lam & Teng Eccentricity Based Model

- $\overline{f_{cc}} = \frac{1}{1+\frac{1}{C_R-0.2}} f_{cc} + \frac{1}{0.8+C_R} f'_c$
- $\overline{\varepsilon_{cu}} = \frac{(\overline{f_{cc}}-f'_c)(\varepsilon_{cc}-0.003)}{f_{cc}-f'_c} + 0.003$
- $f_c = E_c\varepsilon_c - \frac{(E_c-\overline{E_2})^2}{4f'_c}\varepsilon_c^2$ $0 \le \varepsilon_c \le \overline{\varepsilon_t}$
- $f_c = f'_c + \overline{E_2}\varepsilon_c,$ $\overline{\varepsilon_t} \le \varepsilon_c \le \overline{\varepsilon_{ccu}}$
- $\overline{E_2} = \frac{\overline{f_{cc}}-f'_c}{\overline{\varepsilon_{cc}}}$
- $\overline{\varepsilon'_t} = \frac{2f'_c}{E_c-\overline{E_2}}$

22

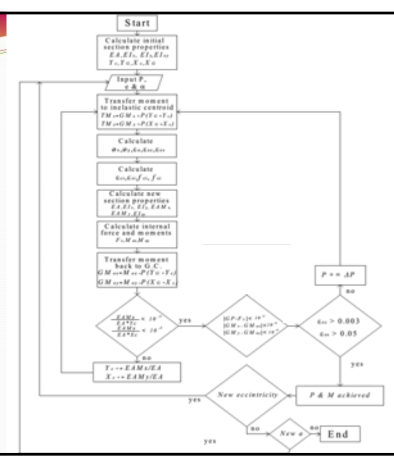

23

KDOT Column Expert

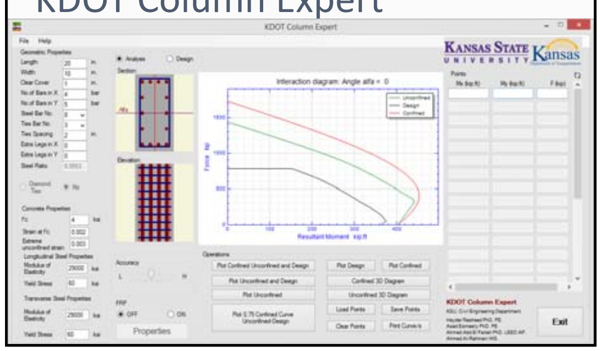

24

Results

- Rocca et al.* provided an experimental results database of rectangular RC columns from the literature.
  - Bousias et al.
  - Memon and Sheikh.
  - Harajli and Rteil.
- Darby et al.

*Rocca, S., Galati, N., and Nanni, A. (2009). "Interaction diagram methodology for design of FRP-confined reinforced concrete columns." Construction & Building Materials, 23(4), 1508-1520.

25

Bousias S, Triantafillou T, Fardis M, Spathis L, O'Regan B. Fiber-reinforced polymer retrofitting of rectangular reinforced concrete columns with or without corrosion. ACI Struct J 2004;101(4):512–20.

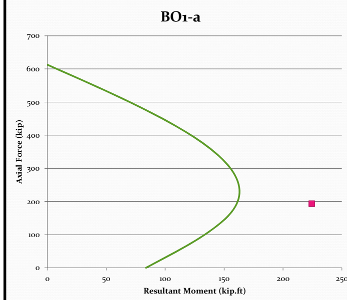

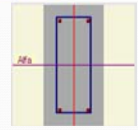

Length = 19.69in
Width = 9.84 in
Cover = 2 in
r_c = 0.52 in
f'_c = 2.65 ksi
f_y = 81.2 ksi
f_{yt} = 41.47 ksi
Long. Steel Dia. = 0.71 in
Lat. Steel Dia. = 0.31 in
Spacing = 7.874 in

26

Bousias S, Triantafillou T, Fardis M, Spathis L, O'Regan B. Fiber-reinforced polymer retrofitting of rectangular reinforced concrete columns with or without corrosion. ACI Struct J 2004;101(4):512–20.

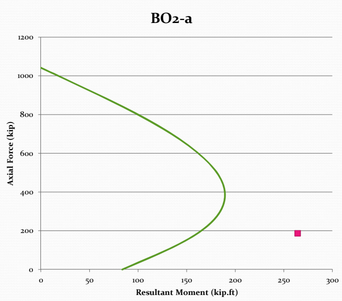

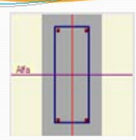

Length = 19.69in
Width = 9.84 in
Cover = 2 in
r_c = 0.52 in
f'_c = 2.62 ksi
f_y = 81.2 ksi
f_{yt} = 41.47 ksi
Long. Steel Dia. = 0.71 in
Lat. Steel Dia. = 0.31 in
Spacing = 7.87 in
E_f = 33350 ksi (CFRP)
ε_{fu} = 1.5%
t_f = 0.005 in
n = 2

27

Bousias S, Triantafillou T, Fardis M, Spathis L, O'Regan B. Fiber-reinforced polymer retrofitting of rectangular reinforced concrete columns with or without corrosion. ACI Struct J 2004;101(4):512–20.

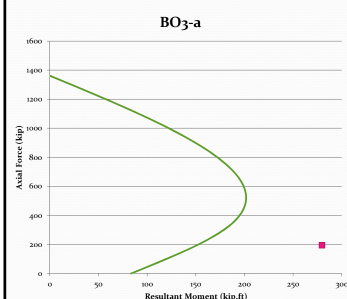

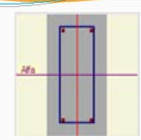

Length = 19.69in
Width = 9.84 in
Cover = 2 in
r_c = 0.52 in
f'_c = 2.6 ksi
f_y = 81.2 ksi
f_{yt} = 41.47 ksi
Long. Steel Dia. = 0.71 in
Lat. Steel Dia. = 0.31 in
Spacing = 7.87 in
E_f = 33350 ksi (CFRP)
ε_{fu} = 1.5%
t_f = 0.005 in
n = 5

28

Bousias S, Triantafillou T, Fardis M, Spathis L, O'Regan B. Fiber-reinforced polymer retrofitting of rectangular reinforced concrete columns with or without corrosion. ACI Struct J 2004;101(4):512–20.

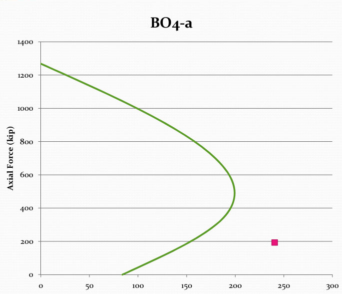

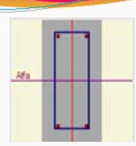

Length = 19.69in
Width = 9.84 in
Cover = 2 in
r_c = 0.52 in
f'_c = 2.71 ksi
f_y = 81.2 ksi
f_{yt} = 41.47 ksi
Long. Steel Dia. = 0.71 in
Lat. Steel Dia. = 0.31 in
Spacing = 7.87 in
E_f = 10150 ksi (GFRP)
ε_{fu} = 3.1%
t_f = 0.0067 in
n = 5

29

Bousias S, Triantafillou T, Fardis M, Spathis L, O'Regan B. Fiber-reinforced polymer retrofitting of rectangular reinforced concrete columns with or without corrosion. ACI Struct J 2004;101(4):512–20.

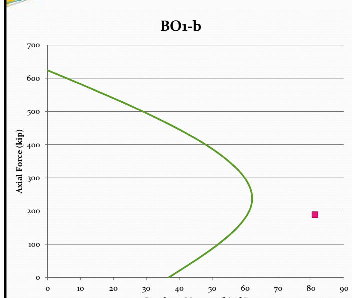

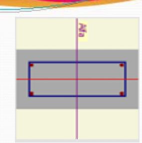

Length = 9.84 in
Width = 19.69 in (weak dir.)
Cover = 2 in
r_c = 0.52 in
f'_c = 2.6 ksi
f_y = 81.2 ksi
f_{yt} = 41.47 ksi
Long. Steel Dia. = 0.71 in
Lat. Steel Dia. = 0.31 in

30

Bousias S, Triantafillou T, Fardis M, Spathis L, O'Regan B. Fiber-reinforced polymer retrofitting of rectangular reinforced concrete columns with or without corrosion. ACI Struct J 2004;101(4):512–20.

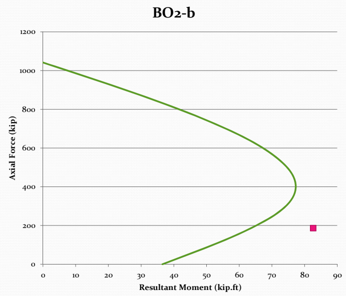

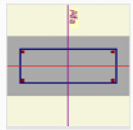

Length = 9.84 in
Width = 19.69 in (weak dir.)
Cover = 2 in
r_c = 0.52 in
f'_c = 2.62 ksi
f_y = 81.2 ksi
f_{yt} = 41.47 ksi
Long. Steel Dia. = 0.71 in
Lat. Steel Dia. = 0.31 in
Spacing = 7.87 in
E_f = 33350 ksi (CFRP)
ε_{fu} = 1.5%
t_f = 0.005 in
n = 2

31

Bousias S, Triantafillou T, Fardis M, Spathis L, O'Regan B. Fiber-reinforced polymer retrofitting of rectangular reinforced concrete columns with or without corrosion. ACI Struct J 2004;101(4):512–20.

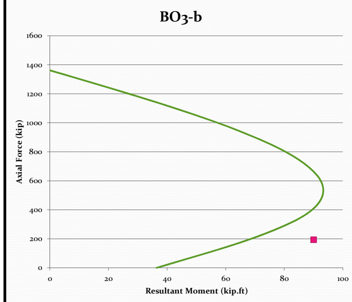

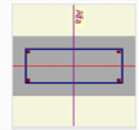

Length = 9.84 in
Width = 19.69 in (weak dir.)
Cover = 2 in
r_c = 0.52 in
f'_c = 2.66 ksi
f_y = 81.2 ksi
f_{yt} = 41.47 ksi
Long. Steel Dia. = 0.71 in
Lat. Steel Dia. = 0.31 in
Spacing = 7.87 in
E_f = 33350 ksi (CFRP)
ε_{fu} = 1.5%
t_f = 0.005 in
n = 5

32

Bousias S, Triantafillou T, Fardis M, Spathis L, O'Regan B. Fiber-reinforced polymer retrofitting of rectangular reinforced concrete columns with or without corrosion. ACI Struct J 2004;101(4):512–20.

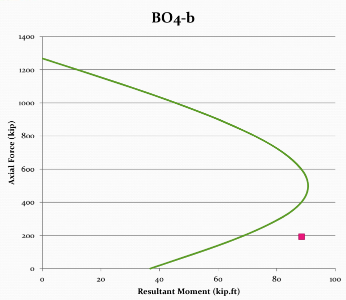

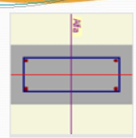

Length = 9.84 in
Width = 19.69 in (weak dir.)
Cover = 2 in
r_c = 0.52 in
f'_c = 2.62 ksi
f_y = 81.2 ksi
f_{yt} = 41.47 ksi
Long. Steel Dia. = 0.71 in
Lat. Steel Dia. = 0.31 in
Spacing = 7.87 in
E_f = 10150 ksi (GFRP)
ε_{fu} = 3.1%
t_f = 0.0067 in
n = 5

33

Memon M, Sheikh S. Seismic resistance of square concrete columns retrofitted with glass fiber-reinforced polymer. ACI Struct J 2005;102(5):774–83.

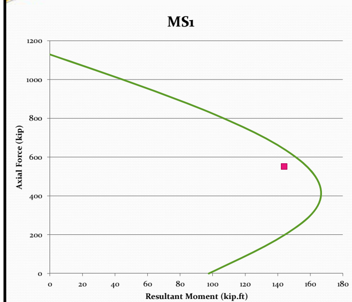

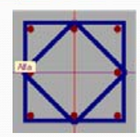

Length = 12 in
Width = 12 in
Cover = 1 in
r_c = 0.64 in
f'_c = 6.15 ksi
f_y = 67.425 ksi
f_{yt} = 66.625 ksi
Long. Steel Dia. = 0.77 in
Lat. Steel = #3
Spacing = 11.8 in

34

Memon M, Sheikh S. Seismic resistance of square concrete columns retrofitted with glass fiber-reinforced polymer. ACI Struct J 2005;102(5):774–83.

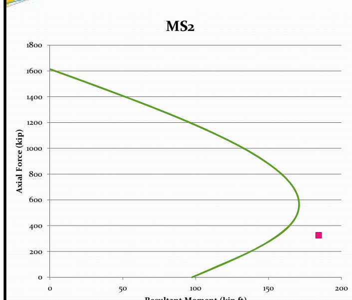

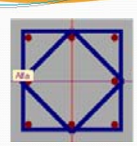

Length = 12 in
Width = 12 in
Cover = 1 in
r_c = 0.64 in
f'_c = 6.16 ksi
f_y = 67.425 ksi
f_{yt} = 66.625 ksi
Long. Steel Dia. = 0.77 in
Lat. Steel = #3
Spacing = 11.8 in
E_f = 2864.33 ksi (GFRP)
ε_{fu} = 2.28%
t_f = 0.05 in
n = 2

35

Memon M, Sheikh S. Seismic resistance of square concrete columns retrofitted with glass fiber-reinforced polymer. ACI Struct J 2005;102(5):774–83.

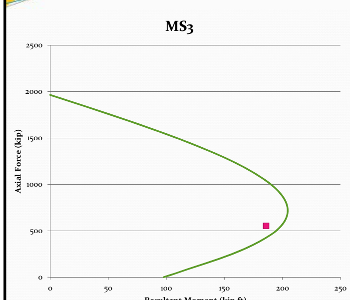

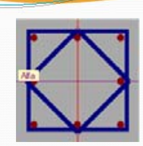

Length = 12 in
Width = 12 in
Cover = 1 in
r_c = 0.64 in
f'_c = 6.19 ksi
f_y = 67.425 ksi
f_{yt} = 66.625 ksi
Long. Steel Dia. = 0.77 in
Lat. Steel = #3
Spacing = 11.8 in
E_f = 2864.33 ksi (GFRP)
ε_{fu} = 2.28%
t_f = 0.05 in
n = 4

36

Memon M, Sheikh S. Seismic resistance of square concrete columns retrofitted with glass fiber-reinforced polymer. ACI Struct J 2005;102(5):774–83.

MS4

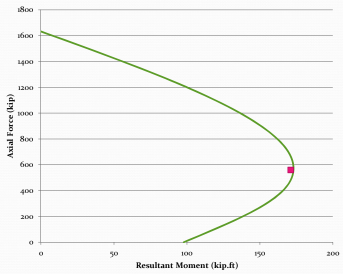

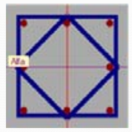

Length = 12 in
Width = 12 in
Cover = 1 in
r_c = 0.64 in
f'_c = 6.28 ksi
f_y = 67.425 ksi
f_{yt} = 66.625 ksi
Long. Steel Dia. = 0.77 in
Lat. Steel = #3
Spacing = 11.8 in
E_f = 2864.33 ksi (GFRP)
ε_{fu} = 2.28%
t_f = 0.05 in
n = 2

Memon M, Sheikh S. Seismic resistance of square concrete columns retrofitted with glass fiber-reinforced polymer. ACI Struct J 2005;102(5):774–83.

MS5

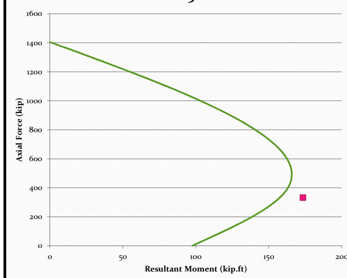

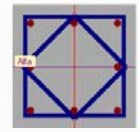

Length = 12 in
Width = 12 in
Cover = 1 in
r_c = 0.64 in
f'_c = 6.34 ksi
f_y = 67.425 ksi
f_{yt} = 66.625 ksi
Long. Steel Dia. = 0.77 in
Lat. Steel = #3
Spacing = 11.8 in
E_f = 2864.33 ksi (GFRP)
ε_{fu} = 2.28%
t_f = 0.05 in
n = 1

Memon M, Sheikh S. Seismic resistance of square concrete columns retrofitted with glass fiber-reinforced polymer. ACI Struct J 2005;102(5):774–83.

MS6

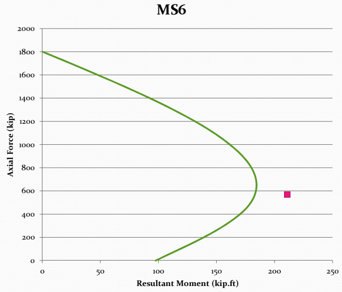

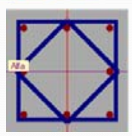

Length = 12 in
Width = 12 in
Cover = 1 in
r_c = 0.64 in
f'_c = 6.41 ksi
f_y = 67.425 ksi
f_{yt} = 66.625 ksi
Long. Steel Dia. = 0.77 in
Lat. Steel = #3
Spacing = 11.8 in
E_f = 2864.33 ksi (GFRP)
ε_{fu} = 2.28%
t_f = 0.05 in
n = 3

Harajli M, Rteil A. Effect of confinement using fiber-reinforced polymer or fiber-reinforced concrete on seismic performance of gravity load-designed columns. ACI Struct J 2004;101(1):47–56.

HR1-a

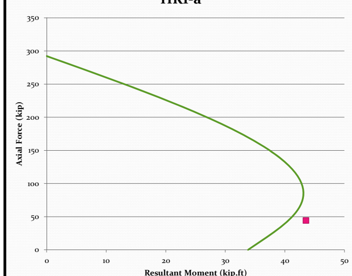

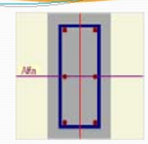

Length = 11.81 in
Width = 5.91 in
Cover = 1 in
r_c = 0.52 in
f'_c = 2.94 ksi
f_y = 77.5 ksi
f_{yt} = 60 ksi
Long. Steel = 6 #4
Lat. Steel Dia.= 0.31 in
Spacing = 5.91 in

Harajli M, Rteil A. Effect of confinement using fiber-reinforced polymer or fiber-reinforced concrete on seismic performance of gravity load-designed columns. ACI Struct J 2004;101(1):47–56.

HR2-a

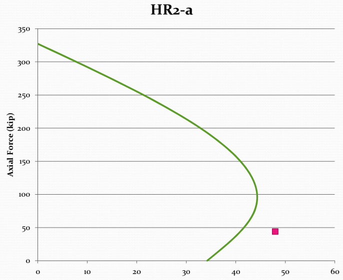

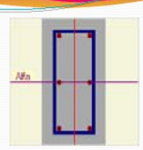

Length = 11.81 in
Width = 5.91 in
Cover = 1 in
r_c = 0.52 in
f'_c = 3.06 ksi
f_y = 77.5 ksi
f_{yt} = 60 ksi
Long. Steel = 6 #4
Lat. Steel Dia.= 0.31 in
Spacing = 5.91 in
E_f = 33350 ksi (CFRP)
ε_{fu} = 1.5%
t_f = 0.005 in
n = 1

Harajli M, Rteil A. Effect of confinement using fiber-reinforced polymer or fiber-reinforced concrete on seismic performance of gravity load-designed columns. ACI Struct J 2004;101(1):47–56.

HR1-b

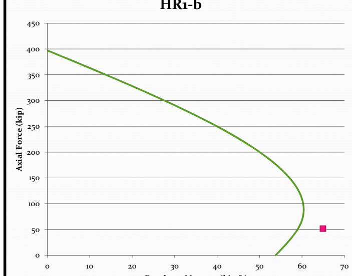

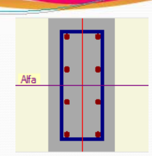

Length = 11.81 in
Width = 5.91 in
Cover = 1 in
r_c = 0.52 in
f'_c = 2.94 ksi
f_y = 81.925 ksi
f_{yt} = 60 ksi
Long. Steel = 8 #5
Lat. Steel Dia.= 0.31 in
Spacing = 5.91 in

Harajli M, Rteil A. Effect of confinement using fiber-reinforced polymer or fiber-reinforced concrete on seismic performance of gravity load-designed columns. ACI Struct J 2004;101(1):47–56.

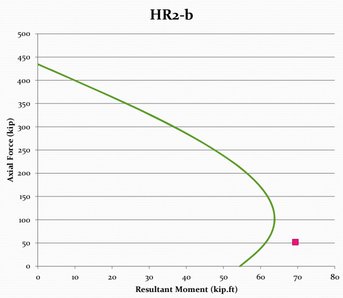

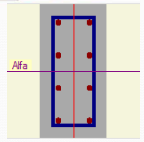

Length = 11.81 in
Width = 5.91 in
Cover = 1 in
r_c = 0.52 in
f'_c = 3.06 ksi
f_y = 81.925 ksi
f_{yt} = 60 ksi
Long. Steel = 8 #5
Lat. Steel Dia.= 0.31 in
Spacing = 5.91 in
E_f = 33350 ksi (CFRP)
ε_{fu} = 1.5%
t_f = 0.005 in
n = 1

43

Darby, A., Coonan, R., Ibell, T., and Evernden, M. (2011). FRP Confined Square Columns under Concentric and Eccentric Loading. Proceedings of the 5th international Advanced composites in construction 2011 conference. (264-275). Chesterfield: NetComposites.

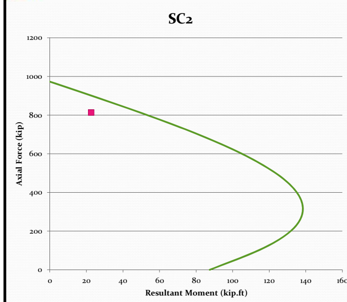

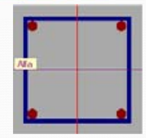

Length = 11.81 in
Width = 11.81 in
Cover = 1 in
r_c = 1.57 in
f'_c = 3.625 ksi
f_y = 79.75 ksi
f_{yt} = 60 ksi
Long. Steel Dia.= 0.98
Lat. Steel= #3
Spacing = 11 in
E_f = 31030 ksi (CFRP)
ε_{fu} = 1.45%
t_f = 0.0063 in
n = 4

44

Darby, A., Coonan, R., Ibell, T., and Evernden, M. (2011). FRP Confined Square Columns under Concentric and Eccentric Loading. Proceedings of the 5th international Advanced composites in construction 2011 conference. (264-275). Chesterfield: NetComposites.

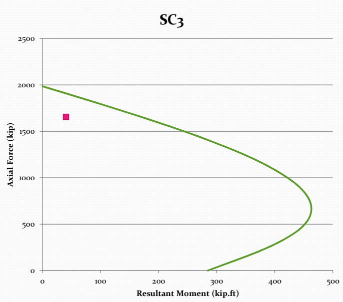

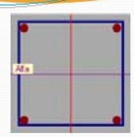

Length = 17.72 in
Width = 17.72 in
Cover = 1 in
r_c = 2.36 in
f'_c = 3.625 ksi
f_y = 79.75 ksi
f_{yt} = 60 ksi
Long. Steel Dia.= 1.39
Lat. Steel= #3
Spacing = 12 in
E_f = 31030 ksi (CFRP)
ε_{fu} = 1.45%
t_f = 0.0063 in
n = 6

45

Conclusions

- In this work, a model was proposed to combine FRP and steel confinement in rectangular reinforced concrete columns.
- The proposed procedure and model were implemented in “KDOT Column Expert” software.
- The proposed model showed good agreement with experimental data.
- The proposed model was shown to be conservative for many cases.

46

Thank you for Listening

Questions?

$$\begin{bmatrix} P \\ M_x \end{bmatrix} = \begin{bmatrix} EA & -EAM_x \\ -EAM_x & EI_x \end{bmatrix} \begin{bmatrix} \varepsilon \\ \phi_x \end{bmatrix}$$

$$f_{cc} = f'_c\left(-1.254 + 2.254\sqrt{1 + \frac{7.94 f'_l}{f'_c}} - 2\frac{f'_l}{f'_c}\right)$$

$$f_{cc} = f_c + 3.3\Psi_f K_a f_l$$

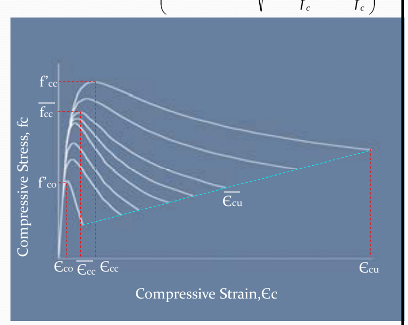

48

- $\overline{\varepsilon_{cu}} = \overline{\varepsilon_{cc}} \left[\frac{\frac{\overline{E_{sec}}}{E_{sec,u}} \bar{r}}{\frac{c}{\overline{\varepsilon_{cc}}} + 1} - \bar{r} + 1 \right]^{\frac{1}{\bar{r}}}$
- $E_{sec,u} = \frac{f_{cu} - f_{cuo}}{\varepsilon_{cu} - 0.003}$
- $c = \frac{f_{cu} - E_{sec,u} * 0.003}{E_{sec,u}}$
- $110\rho_s = \int_0^{\varepsilon_{cu}} f_c \, d\varepsilon + \int_0^{\varepsilon_{cu}} f_{sl} \, d\varepsilon - 0.017\sqrt{f_c'}$